Transport properties of normal liquid helium: Comparison of various methodologies

Eran Rabani
School of Chemistry, The Sackler Faculty of Exact Sciences, Tel Aviv University, Tel Aviv 69978, Israel

Goran Krilov,[a] David R. Reichman, and B. J. Berne
Department of Chemistry, Columbia University, New York, New York 10027

(Received 12 August 2005; accepted 9 September 2005; published online 10 November 2005)

We revisit the problem of self-diffusion in normal liquid helium above the λ transition. Several different methods are applied to compute the velocity autocorrelation function. Since it is still impossible to determine the exact result for the velocity autocorrelation function from simulation, we appeal to the computation of short-time moments to determine the accuracy of the different approaches at short times. The main conclusion reached from our study is that both the quantum mode-coupling theory and the numerical analytic continuation approach must be regarded as a viable and competitive methods for the computation of dynamical properties of quantum systems. © *2005 American Institute of Physics*. [DOI: 10.1063/1.2109927]

I. INTRODUCTION

The study of time correlation functions in condensed phases has occupied a central role in modern physics and physical chemistry. Indeed, since all linear response properties of a condense phase system may be obtained through the study of time correlation functions, it is difficult to overstate their importance.[1] For systems that obey classical mechanics, molecular-dynamics simulations may be performed to compute the time correlation functions.[2,3] The only approximate element of such calculations is the form of the potential energy that is used to calculate forces. At the present time there is no practical analog of molecular dynamics for the calculation of real-time dynamics in quantum many-body systems. This has lead to the development of several approximate schemes for computing dynamical correlations in quantum condensed phase systems.[4–16] The main goals in the development of such methods are accuracy and efficiency. While efficiency is easily gauged, accuracy is difficult to access.

One class of approximate techniques relies on attempting to infer the real-time dynamics from the dynamics of closed, imaginary-time paths. In the centroid molecular-dynamics (CMD) technique,[11,17–28] the center of mass of such paths forms the dynamical object that is needed for the computation of time correlation functions.[18] In the case of the ring polymer molecular dynamics (RPMD),[29,30] the entire thermal path is used to compute dynamical correlations. The RPMD is identical to the CMD for the standard velocity and position autocorrelation functions, and in fact it can be shown that the RPMD formalism can be obtained using adiabatic CMD. It differs from CMD for correlation functions involving nonlinear operators in position or momenta. Both methods have the advantage of relative efficiency so that they may be applied to complex molecular systems, and both are exact for the harmonic oscillator if at least one of the operators in the correlation function is a linear function of position or momentum. However, since there is no direct link between imaginary-time and real-time dynamics, there is no *a priori* reason that the dynamics should be accurate.[31,32]

Another set of approaches is based on the semiclassical (SC), $\hbar \to 0$ limit.[4–9,33,34] These approaches use real classical trajectories to compute the quantum time correlation functions. The simpler versions of this type of approach are quite efficient computationally,[15,35–41] and may be applied to large, complex systems, while the less approximate versions are much more difficult to implement and converge. All levels of semiclassical techniques of this type are amenable to the correlation functions of operators of arbitrary nonlinearity. Since the expansion in $\hbar$ has zero radius of convergence, it is, in principle, impossible to "correct" such approaches.[42,43] In particular, coherent tunneling effects cannot be captured and corrections in powers of $\hbar$ cannot cure this ill. Like all methods discussed here, it is difficult to access the accuracy of the dynamics, even at short times. Indeed, as discussed by Golosov and Reichman,[44] crude semiclassical methods my fail to capture the short-time moments due to the neglect of proper commutation constraints.

An approach we have adopted in recent years is based on a quantum version of mode-coupling theory (QMCT).[16,45–52] Here, the path-integral simulation is used only for the computation of the static structural information[16,53] that is needed for the self-consistent solution of the nonlinear mode-coupling equations. The method may be used to compute arbitrarily complex correlation functions. From the stand point of field theory,[54] the method may be seen as a self-consistent resummation of diagrams that involve no vertex correction. In this light, the approach is similar to the "random-phase approximation" (RPA) used to treat electronic systems.[54,55] Thus, while QMCT involves no direct semiclassical expansion in $\hbar$, it may be seen as a semiclassical theory much in the way the RPA is a semiclassical

[a]Present address: Department of Chemistry, Boston College, Merkert Center, 2609 Beacon St., Chestnut Hill, MA 02467.

theory of the electron gas.[56,57] Of all of the direct, real-time dynamical approaches outlined above, QMCT is perhaps the cheapest from the computational perspective, since it is always less demanding to compute static quantities than to run dynamics of any kind. On the other hand, the formulation of QMCT for complex systems, such as molecular systems with internal degrees of freedom, is complicated.[58,59] Thus, methods such as RPMD and CMD have an advantage over QMCT in this regard. Furthermore, the SC, CMD, and RPMD methods are exact in the classical limit, while QMCT is not (it reduces to the classical mode-coupling theory[60–62]). Nevertheless, when compared to experiments probing both the single particle and collective dynamics of quantum liquids, QMCT appears to be competitive with the other methods discussed above. In some cases, QMCT appears to be the method of choice.[49]

Another class of approaches that do not involve the direct simulation of real-time dynamics are those that utilize analytic continuation of imaginary time data.[10,14,63–74] In principle, these methods are exact, but limitations on the quality of simulated imaginary time trajectories, and the ill-posed nature of the analytic continuation render these approaches as uncontrolled as the methods discussed above. Perhaps the most reliable of these techniques is the maximum entropy (ME) approach.[14] ME uses Bayesian techniques to control the instability of the inversion. ME must be used with care when several various important energy scales in a physical process are similar in magnitude.[75] Regardless of this intrinsic resolution issue, ME is useful for estimating the bandwidth of the quantum dynamics.[10]

In this paper, we study the transport properties of liquid helium at relatively low temperatures. The temperature range that we study is above the λ temperature, and thus exchange effects may be neglected.[76] However, the present system is in a deeper quantum regime than the previous study of transport properties in other quantum liquids.[31,73,77] While the diffusion coefficients may be accurately computed by the variety of methods discussed above, all of the methods appear to give noticeably different quantitative behavior with regard to the full time dependence of the velocity correlation function at the lower temperature studied.[31,73] We will see that the same is true for helium. Since it is still impossible to determine the exact result from simulation, we appeal to the computation of short-time moments to determine the accuracy of the different approaches at short times. This exercise in no way can confirm the accuracy of a given approach at all times, however, discrepancy with computed short-time moments points towards the possible inaccuracy. The conclusion reached from our study is that, as far as the available data are concerned, QMCT and numerical analytic continuation (NAC) must be regarded as a viable and competitive methods for the computation of dynamical properties of quantum systems.

The paper is organized as follows: In Sec. II we discuss various approaches we have developed to computing the velocity correlation function in quantum fluids. In Sec. III we apply these methods to the study of normal liquid helium. We also discuss the application of CMD and the semiclassical approach of Nakayama and Makri to the same problem. In Sec. IV we conclude.

II. VELOCITY AUTOCORRELATION FUNCTION

In this section we outline two methods that we have developed for computing the velocity autocorrelation function and the self-diffusion constant in a quantum liquid. The first is based on a quantum mode-coupling theoretical approach and the other is based on a numerical analytic continuation of imaginary path-integral Monte Carlo (PIMC) data to real time.

A. Quantum mode-coupling theory

Within the framework of a QMCT the computation of the velocity autocorrelation function is accomplished by augmenting a quantum generalized Langevin equation (QGLE) for the Kubo transform of this correlation function.[78–81] The exact solution of this QGLE can be obtained only for a limited class of simple systems. For the general many-body case, however, approximations must be introduced. In this subsection we summarize the approach we have developed to study the transport properties of quantum liquid based on the above scheme. We briefly derive a QGLE for the velocity autocorrelation function and summarize the approximations used to solve the QGLE. A more complete discussion can be found elsewhere.[16,47,49]

We begin with the definition of the projection operator P_κ:

$$P_\kappa = \frac{\langle v, \cdots \rangle}{\langle v, v_\kappa \rangle} v_\kappa, \tag{1}$$

where

$$v_\kappa = \frac{1}{\beta\hbar} \int_0^{\beta\hbar} d\lambda e^{-\lambda H} v e^{\lambda H} \tag{2}$$

is the Kubo transform[82] of the velocity operator $v=p/m$ of a representative liquid particle along a chosen Cartesian direction, H is the Hamiltonian of the system, $\beta=1/(K_B T)$, and $\langle \cdots \rangle$ denote a quantum-mechanical ensemble average. In the above equations the notation κ implies that the quantity under consideration involves the Kubo transform defined in Eq. (2). Using the standard procedure it is straightforward to show that the QGLE for the Kubo transform of the velocity autocorrelation function, $C_v^\kappa(t)=\langle v v_\kappa(t) \rangle$, is given by the *exact* equation,

$$\dot{C}_v^\kappa(t) = -\int_0^t dt' K^\kappa(t') C_v^\kappa(t-t'), \tag{3}$$

where $\dot{C}_v^\kappa(t)=\partial C_v^\kappa(t)/\partial t$, and the Kubo transform of the memory kernel, $K^\kappa(t)$, is given by the exact equation,

$$K^\kappa(t) = \frac{1}{\langle v, v_\kappa \rangle} \langle \dot{v}, e^{i(1-P_\kappa)\mathcal{L}t} \dot{v}_\kappa \rangle. \tag{4}$$

In the above equation $\mathcal{L}=(1/\hbar)[H,]$ is the quantum Liouville operator.

To obtain the memory kernel, which involves the projected propagation operator $e^{i(1-P_\kappa)\mathcal{L}t}$, we approximate the memory kernel as $K^\kappa(t)=K_b^\kappa(t)+K_{\mathrm{MCT}}^\kappa(t)$. The fast decaying binary term, $K_b^\kappa(t)$, is obtained from a short-time expansion of the exact Kubo transform of the memory function, and is given by

$$K_b^\kappa(t) = K^\kappa(0) f(t/\tau), \tag{5}$$

where the lifetime $\tau=[-\ddot{K}^\kappa(0)/2K^\kappa(0)]^{-1/2}$, $K^\kappa(0)=\langle \dot{v}, \dot{v}_\kappa\rangle/\langle v, v_\kappa\rangle$, and $\ddot{K}(\kappa)^0=-\langle \ddot{v}, \ddot{v}_\kappa\rangle/\langle v, v_\kappa\rangle+[K^\kappa(0)]^2$. The shape of the function $f(x)$ is taken to be a Gaussian $\exp(-x^2)$ or $\mathrm{sech}^2(x)$. Both forms have been used in the study of classical liquids,[60] and are exact to second order in time.

The slowly decaying mode-coupling term, $K_{\mathrm{MCT}}^\kappa(t)$, is given within a simple closure by

$$K_{\mathrm{MCT}}^\kappa(t) \approx \frac{1}{2\pi^2 n\langle v, v_\kappa\rangle}\int_0^\infty dq q^2 |V^\kappa(\mathbf{q})|^2 [F_s^\kappa(q,t) - F_{s,b}^\kappa(q,t)]F^\kappa(q,t). \tag{6}$$

In the above equation n is the number density, $F^\kappa(q,t)$ is the Kubo transform of the intermediate scattering function, and $F_s^\kappa(q,t)$ is the Kubo transform of the self-intermediate scattering function. The binary term of the Kubo transform of the self-intermediate scattering function, $F_{s,b}^\kappa(q,t)$, is obtained from a short-time expansion of $F_s^\kappa(q,t)$ similar to the expansion used for the binary term of $K^\kappa(t)$. The subtraction of this term in Eq. (6) is done to prevent over counting the total memory kernel at short times (since the binary portion of the memory kernel is exact to second order in time). The vertex in Eq. (6) is given by

$$V^\kappa(\mathbf{q}) = \frac{\langle b(\mathbf{q})\dot{v}_\kappa\rangle}{NF_s^\kappa(q,0)F^\kappa(q,0)}, \tag{7}$$

where N is the number of particles, and $b(\mathbf{q})=\Sigma_{j\neq 1}^N e^{i\mathbf{q}\cdot(\mathbf{r}_1-\mathbf{r}_j)}$ is related to the single-particle and number variable density operators.

To obtain both portions of the memory kernel one requires as input the values of the memory function at $t=0$, its second time derivative at $t=0$, and the vertex. While these properties can be obtained from *static* equilibrium input, however, they involve thermal averages over operators that combine positions and momenta of all particles. The approach we adopt in the present study to calculate these averages is based on a recent method that we have developed which uses a path-integral Monte Carlo technique and is suitable for thermal averages of such operators for a many-body system.[53]

In addition to these static properties, one requires also the Kubo transforms of the *time-dependent* intermediate and self-intermediate scattering functions. The former is obtained from an analytic continuation approach[51] which for the case of normal liquid helium provides numerically accurate results.[67] The analytic continuation results for $F^\kappa(q,t)$ are shown in the left panels of Fig. 1 for several values of q. The simulation details used to generate these results are described below in Sec. III. The right panels of Fig. 1 show the corresponding dynamics structure factors, $S(q,\omega)=\int_{-\infty}^\infty dt e^{i\omega t}F(q,t)$, along with the experimental results at 4.2 K.[83] The agreement between the analytic continuation approach and the experiments is remarkable.[67] For the self-intermediate scattering function we assume a Gaussian approximation,

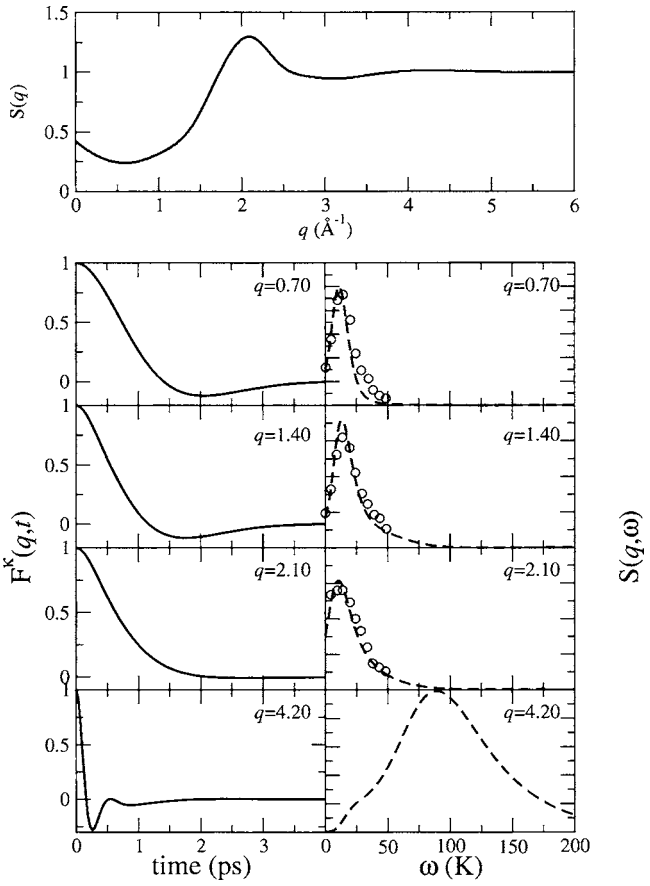

FIG. 1. Plots of the static structure factor (upper panel), Kubo transform of the intermediate scattering function (left panels), and the dynamic structure factor (right panels) for normal liquid helium at $T=4$ K and $\rho=0.018\,73$ Å^{-3}. The solid lines are the results obtained from the NAC method and the open circles are the experimental results at 4.2 K from Ref. 83.

$$F_s^\kappa(q,t) = F_s^\kappa(q,0)\exp\left\{-q^2\int_0^t dt' C_v^\kappa(t')(t-t')\right\}, \tag{8}$$

where the Kubo transform $F_s^\kappa(q,0)$ can be obtained from a static equilibrium PIMC method.

B. Analytic continuation of the velocity autocorrelation function

An alternative approach to the quantum mode-coupling theory is based on the numerical analytic continuation of imaginary-time data. Following the approach described in our previous study on liquid parahydrogen,[73] we introduce $D(\omega)$,

$$D(\omega) = \int_{-\infty}^\infty dt e^{i\omega t} C_v(t), \tag{9}$$

as the power spectrum of the quantum velocity autocorrelation function given by

$$C_v(t) = \frac{1}{Z}\mathrm{Tr}(e^{-\beta H}e^{iHt}ve^{-iHt}v), \tag{10}$$

where $\hbar=1$ and $Z=\mathrm{Tr}\, e^{-\beta H}$ is the partition function, $\beta=1/k_bT$ is the inverse temperature, and as before, v is the velocity operator of a tagged particle in the liquid along a chosen direction. The self-diffusion constant is then given by the Green-Kubo relation as the zero-frequency value of $D(\omega)/2$.[84]

The power spectrum $D(\omega)$ is also related to the imaginary-time velocity autocorrelation function $G_v(\tau)$,

$$G_v(\tau) = \frac{1}{Z}\mathrm{Tr}(e^{-\beta H}e^{\tau H}ve^{-\tau H}v), \tag{11}$$

obtained by a Wick rotation $t\rightarrow -i\tau$, through a two-sided Laplace transform,

$$G_v(\tau) = \frac{1}{2\pi}\int_0^\infty d\omega[e^{-\omega\tau}+e^{(\tau-\beta)\omega}]D(\omega), \tag{12}$$

where t, $\tau\geqslant 0$, and we have used the detailed balance relation $D(-\omega)=e^{-\beta\omega}D(\omega)$.

The imaginary-time correlation function can be computed in a straightforward fashion using an appropriate path-integral Monte Carlo simulation technique.[53,85,86] The path-integral parametrization we use to obtain $G_v(\tau)$ is identical to the one used in our previous work in liquid parahydrogen.[73] The result to lowest order in $\epsilon=\beta/P$, where P is the number of Trotter slices, is

$$G_v(\tau_j) = \delta_{j1}\frac{1}{3m\epsilon} - \frac{1}{N\epsilon^2}\sum_{\alpha=1}^{N}\int d\mathbf{r}_1\cdots d\mathbf{r}_P P(\mathbf{r}_1,\ldots,\mathbf{r}_P) \times(\mathbf{r}_\alpha^j-\mathbf{r}_\alpha^{j-1})\cdot(\mathbf{r}_\alpha^2-\mathbf{r}_\alpha^1). \tag{13}$$

As before, N is the total number of liquid particles, $\mathbf{r}_j$ is a shorthand notation for the position vector of all liquid particles associated with bead j, $\mathbf{r}_\alpha^j$ is the position vector of liquid particle α of bead j, and $P(\mathbf{r}_1,\ldots,\mathbf{r}_P)$ is the regular sampling function used in the standard *cyclic* PIMC method (with $r_0=r_P$).

The power spectrum $D(\omega)$ then obtained by a numerical inversion of the integral equation (12), which completes the analytic continuation procedure. The real-time velocity correlation function can then be computed from $D(\omega)$ via a simple Fourier transform. As mentioned above, the experimentally observable self-diffusion constant can be obtained from the zero mode value $D=D(0)/2$.

The analyticity of $G_v(\tau)$ on $0<\tau<\beta$ ensures the existence and uniqueness of the inversion. However, the singular nature of the integral kernel and the finite statistical error associated with the $G_v(\tau)$ introduce a significant numerical instability in the inversion. As a consequence, a direct approach to the inversion would lead to an uncontrollable amplification of the statistical noise in the data for $G_v(\tau)$, resulting in an infinite number of solutions that satisfy Eq. (12).

C. Maximum entropy numerical analytic continuation

We used the Bayesian-based ME method to control the instability of the inversion. The approach has been described extensively in our previous work, and we outline it here briefly for completeness. We rewrite the integral equation (12) as

$$G(\tau) = \int d\omega K(\tau,\omega)A(\omega), \tag{14}$$

where $G(\tau)\equiv G_v(\tau)$ represents the data (in this case the imaginary-time velocity autocorrelation function), $K(\tau,\omega)=e^{-\omega\tau}+e^{(\tau-\beta)\omega}$ is the singular kernel, and $A(\omega)$ is the solution, referred to as the map [corresponding to $D(\omega)$]. Maximum entropy principles provide a way to choose the most probable solution which is consistent with the data through the methods of Bayesian inference. Typically, the data are known only at a discrete set of points $\{\tau_j\}$, and we likewise seek the solution at a discrete set of points $\{\omega_k\}$. The ME method selects the solution which maximizes the posterior probability, or the probability of the solution $\mathbf{A}$ given a data set $\mathbf{G}$.

Using Bayesian ideas, it can be shown that the posterior probability[63,87] is appropriately given by

$$\mathcal{P}(\mathbf{A}|\mathbf{G}) \propto \exp(\alpha S-\chi^2/2) = e^{Q}. \tag{15}$$

Here χ^2 is the standard mean-squared deviation from the data

$$\chi^2 = \sum_{j,k}\left(G_j-\sum_l K_{jl}A_l\right)[C^{-1}]_{jk}\left(G_k-\sum_l K_{kl}A_l\right), \tag{16}$$

where C_{jk} is the covariance matrix,

$$C_{jk} = \frac{1}{M(M-1)}\sum_{l=1}^{M}(\langle G_j\rangle - G_j^{(l)})(\langle G_k\rangle - G_k^{(l)}), \tag{17}$$

with M being the number of measurements.

S is the information entropy, the form of which is axiomatically chosen to be

$$S = \sum_k \Delta\omega\left(A_k-m_k-A_k\ln\frac{A_k}{m_k}\right). \tag{18}$$

In this formulation the entropy is measured relative to a default model $m(\omega)$ which can contain prior information about the solution, and α is a positive regularization parameter controlling the smoothness of the map. Large values of α lead to a result primarily determined by the entropy function and hence the default model. Small α in turn lead to a map determined mostly by the χ^2 and thus to a closer fitting of the data. The principal drawback is that, along with the data, the errors would be fit as well.

The ME method was used to numerically invert the integral in Eq. (12). We use a flat prior to $(m(\omega))$, which satisfies a known sum rule, i.e., the integral over $D(\omega)$, and α is determined according to the L-curve method.[88]

III. APPLICATION TO NORMAL LIQUID HELIUM

The dynamic response of liquid helium above the λ transition remains a challenge to theoretical and computational schemes. Despite the fact that helium above the λ transition

may be treated as a Boltzmann particle, due to the relatively low temperature ($\approx$4 K) it still exhibits some of the hallmarks of a highly quantum liquid.[76] In addition, theoretical treatments applicable to low- or high-density fluids breakdown at the intermediate density regime, characteristic of normal liquid helium.[76]

Several different numerical methods have been applied recently to study the dynamical properties of normal liquid helium.[32,89,90] In this section we revisit the problem of transport in normal liquid helium and compare the results of the different semiclassical methods with the results of the quantum mode-coupling theory and the numerical analytical continuation method described above. Discrepancies between the semiclassical methods and the other approaches observed at short times are discussed, and the results are compared to a numerically exact short-time expansion of the real-time velocity autocorrelation function.

In order to obtain the static input required for the quantum mode-coupling approach and the imaginary time data required for the numerical analytic continuation approach, we have performed PIMC simulations in the *NVT* ensemble at $T=4$ K and $\rho=0.018\,73$ Å^{-3}. A total of $N=256$ ($N=108$ for the QMCT results) helium atoms were simulated for a total of 6×10^6 Monte Carlo moves using the staging algorithm.[91] The number of Trotter slices was $P=100$, ensuring the convergence of structural properties. The interaction between helium atoms was modeled by the well-established Aziz potential.[92]

The static input generated from the PIMC simulations combined with the Kubo transform of the intermediate scattering function obtained from the analytic continuation approach was then used to generate the memory kernel for the QGLE of the velocity autocorrelation function. Using $F^{\kappa}_{s,b}(q,t)$ as an initial guess for the Kubo transform of the self-intermediate scattering function, we have solved Eqs. (3), (5), (6), and (8) self-consistently to obtain $C^{\kappa}_{v}(t)$. Typically, less than ten iterations were required to converge the self-consistent cycles.

The PIMC simulations were also used to generate the imaginary-time data for the ME numerical analytic continuation procedure. The required covariance matrices were computed by block averaging the Monte Carlo data, and a singular value decomposition technique was used to decorrelate the statistical noise of each data point.[10] The ME procedure was then used to determine the frequency-dependent diffusion constant corresponding to each state point by inverting Eq. (12). The *L*-curve method yielded the value of the regularization parameter $\alpha=1\times10^7$, which produced a stable solution. We found that the results of the inversion are not sensitive to the exact choice of α over a relatively wide range.

In Fig. 2 we plot the power spectrum of the velocity autocorrelation function for normal liquid helium. The results obtained from the QMCT and from the NAC approach are compared with the recent results obtained by centroid molecular dynamics[89] (CMD) and by a semiclassical (SC) approach.[32] All results give similar diffusion constants (NAC result is slightly higher than the others), as can be seen from the value of $D(\omega)$ at $\omega=0$.

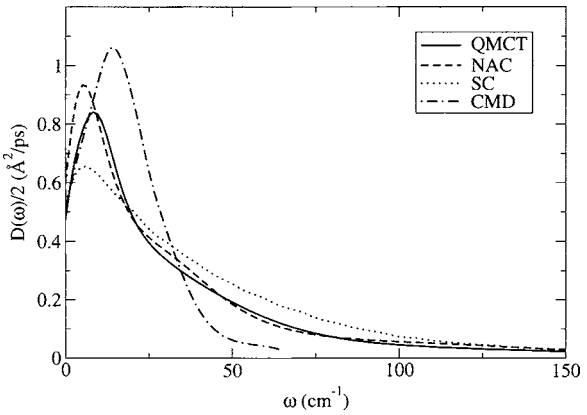

FIG. 2. A plot of the frequency-dependent diffusion constant for normal liquid helium at $T=4$ K and $\rho=0.018\,73$ Å^{-3}. The solid, dashed, dotted, and dot-dashed lines are the results from quantum mode-coupling theory (QMCT), numerical analytic continuation (NAC) method, Nakayama and Makri semiclassical (SC) approach (Ref. 32, $\rho=0.019\,32$ Å^{-3}), and the centroid molecular-dynamics (CMD) simulation approach (Ref. 89), respectively.

Common to all methods is that the power spectrum is asymmetric and is characterized by a single frequency peak. This is precisely the limit in which the NAC method should provide accurate results.[49,51] The overall agreement between the QMCT and NAC methods is quite good over the entire frequency range. The position of the frequency peak and its width are comparable in both cases. In comparison, the position of the peak is somewhat higher and the decay of $D(\omega)$ at large ω is slightly faster for the CMD results. The overall shape $D(\omega)$ calculated from the SC method is qualitatively similar to that obtained from the QMCT and NAC methods, however, the width obtained from the SC method is somewhat larger.

A similar picture emerges when the results for the velocity autocorrelation functions are compared in the time domain. In Fig. 3 we show the normalized velocity autocorrelation functions obtained from the QMCT, NAC, and SC results of Nakayama and Makri.[32] The real-time velocity autocorrelation function in the QMCT and the NAC methods was computed directly from the power spectrum by taking the inverse of Eq. (9). The agreement between the QMCT and the NAC at short times is excellent. The SC result decays somewhat faster than the other two methods. At longer times the velocity autocorrelation function computed from the QMCT becomes slightly negative, while the NAC method and the SC approach are positive for all times.

The faster decay of the SC result compared to the QMCT and the NAC methods is consistent with the picture in frequency space, where we find that the power spectrum is somewhat broader for the SC result. The advantage of comparing the results in the time domain is that at short times, one can compute the exact expansion of the real part of the velocity autocorrelation function by calculating the even time moments directly from the PIMC simulations. This comparison is given in Table I. In all three cases, the zero time value of $C_v(t)$ is within 10% from the numerically exact result (PIMC). The QMCT is exact at $t=0$ for the Kubo transform of the velocity autocorrelation function, but is not

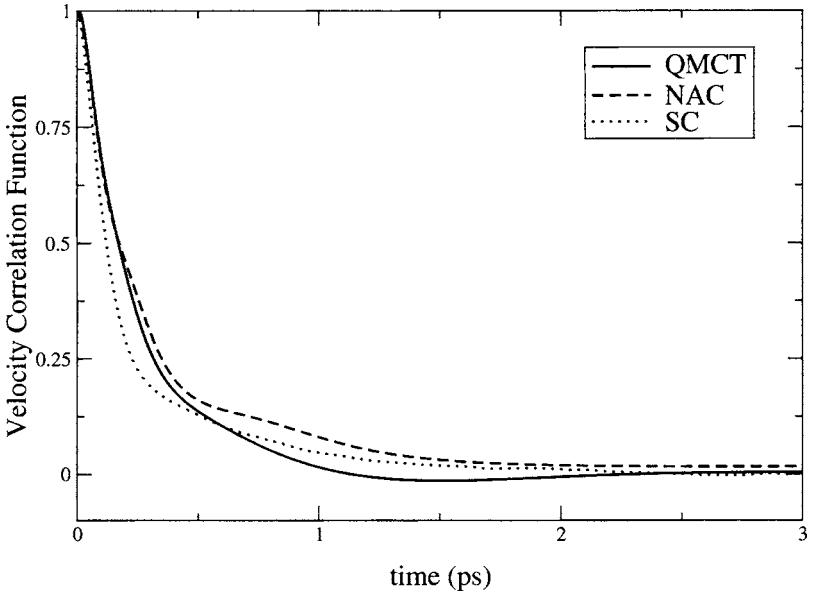

FIG. 3. A plot of the real part of the normalized velocity autocorrelation function for normal liquid helium $T=4$ K and $\rho=0.018\,73$ Å^{-3}. The solid, dashed, and dotted lines are the results from QMCT, NAC method, and the Nakayama and Makri SC approach (Ref. 32, $\rho=0.019\,32$ Å^{-3}), respectively.

exact for the velocity autocorrelation function itself. Within the error bars of the inversion process, the NAC method is the most accurate approach for $C_v(0)$. The SC approach also provides a very good estimate of $C_v(0)$. This is a result of the use of an exact representation of the thermal density operator.

Turning to discuss the results for the higher time moments of $C_v(t)$, it is clear that the SC result overestimates the second and fourth moments by nearly a factor of 2 and nearly a factor of 3, respectively, while both the QMCT and NAC methods are in reasonable agreement with the exact PIMC results. Thus, based on this analysis, we expect the SC result to decay faster than the expected exact result, as indeed is observed in Fig. 3. On the other hand, the agreement between the QMCT and NAC methods at short times is not surprising based on the short-time moment analysis. Furthermore, we expect the QMCT and NAC methods to better approximate the exact result at early stages of the decay of the velocity autocorrelation function.

The differences between the SC result and QMCT and NAC at short times is unexpected. For parahydrogen the results agree much better at short times for the higher temperature studied.[31] One possible explanation is related to the fact that the moments are calculated in the frequency domain. This is necessary for the QMCT and the NAC methods, for SC one can obtain the moments directly from the the real-time data, however, this requires higher time resolution. Other possible explanations for the observed discrepancy is the smaller system size used in the SC method and perhaps also convergence issues with respect to averaging.[93]

TABLE I. Even time moments to fourth order of the velocity autocorrelation in atomic units. The PIMC result is the numerically exact result.

	QMCT	NAC	SC	PIMC
$C_v(0)(10^{-9})$	4.69	4.36	4.53	4.39
$\ddot{C}_v(0)(10^{-16})$	3.39	3.15	5.11	3.91
$\ddot{C}_v(0)(10^{-22})$	2.02	1.88	5.53	1.86

IV. CONCLUSIONS

In this paper we apply several approaches to the study of single-particle motion in liquid helium above the λ transition temperature. While the helium atoms may be treated as the Boltzmann particles under these conditions, the system exhibits strong thermal tunneling and zero-point effects, making it a challenging case for theoretical study. In particular, a larger number of imaginary-time Trotter slices are needed to converge the structural quantities at the thermodynamic state point studied in this work than in the previous application such as parahydrogen and orthodeuterium. We find that the SC, QMCT, and NAC approaches provide a largely consistent picture for the full frequency-dependent diffusion constant $D(\omega)$, while the CMD result differs markedly. Differences in the frequency domain between SC, QMCT, and NAC appear more strikingly in the time domain. The short-time decay of the velocity correlation function as computed via the SC approach decays faster than that computed in the QMCT or NAC approximations. This faster decay is consistent with the fact that the short-time moments extracted from the SC approach differ from those computed from a direct PIMC calculation, while the moments extracted from QMCT and NAC are largely consistent with these values. While these results do not constitute a direct verification of the accuracy of QMCT and NAC to the study of quantum liquid, the results presented demonstrate that these methods are competitive with all other approaches that are currently available.

ACKNOWLEDGMENTS

The authors would like to thank Nancy Makri for providing the results for the velocity autocorrelation function obtained from a semiclassical approach, and Gregory A. Voth and Tyler D. Hone for stimulating discussions. This work was supported by The Israel Science Foundation [Grant No. 31/02-1 to one of the authors (E.R.)] and by the National Science Foundation [Grant No. CHE-03-16896 to another author (B.J.B.)]. Another author (D.R.R.) is an Alfred P.

Sloan Foundation Fellow and a Camille Dreyfus Teacher-Scholar.

[1] D. Forster, *Hydrodynamics, Fluctuations, Broken Symmetry, and Correlation Functions* (Addison-Wesley, New York, 1990).
[2] M. P. Allen and D. J. Tildesley, *Computer Simulation of Liquids* (Oxford University Press, Oxford, 1987).
[3] D. Frenkel and B. Smit, *Understanding Molecular Simulations: Algorithms and Applications* (Academic, San Diego, 2002).
[4] J. C. Tully, Annu. Rev. Phys. Chem. **31**, 319 (1980).
[5] E. J. Heller, Acc. Chem. Res. **14**, 268 (1981).
[6] W. H. Miller, Science **233**, 171 (1986).
[7] R. B. Gerber and M. A. Ratner, Adv. Chem. Phys. **74**, 97 (1988).
[8] D. F. Coker, in *Computer Simulation in Chemical Physics*, edited by M. P. Allen and D. J. Tildesley (Kluwer Academic, Dordrecht, 1993), p. 315.
[9] M. F. Herman, Annu. Rev. Phys. Chem. **45**, 83 (1994).
[10] M. Jarrell and J. E. Gubernatis, Phys. Rep. **269**, 134 (1996).
[11] G. A. Voth, Adv. Chem. Phys. **93**, 135 (1996).
[12] S. A. Egorov, E. Rabani, and B. J. Berne, J. Phys. Chem. B **103**, 10978 (1999).
[13] N. Makri, Annu. Rev. Phys. Chem. **50**, 167 (1999).
[14] G. Krilov, E. Sim, and B. J. Berne, Chem. Phys. **268**, 21 (2001).
[15] W. H. Miller, J. Phys. Chem. A **105**, 2942 (2001).
[16] E. Rabani and D. R. Reichman, Annu. Rev. Phys. Chem. **56**, 157 (2005).
[17] J. Cao and G. A. Voth, J. Chem. Phys. **100**, 5106 (1994).
[18] S. Jang and G. A. Voth, J. Chem. Phys. **111**, 2371 (1999).
[19] S. J. Jang and G. A. Voth, J. Chem. Phys. **111**, 2357 (1999).
[20] P. N. Roy and G. A. Voth, J. Chem. Phys. **110**, 3647 (1999).
[21] P. N. Roy, S. J. Jang, and G. A. Voth, J. Chem. Phys. **111**, 5303 (1999).
[22] K. Kinugawa, Chem. Phys. Lett. **292**, 454 (1998).
[23] F. J. Bermejo, K. Kinugawa, C. Cabrillo, S. M. Bennington, B. Fak, M. T. Fernandez-Diaz, P. Verkerk, J. Dawidowski, and R. Fernandez-Perea, Phys. Rev. Lett. **84**, 5359 (2000).
[24] D. R. Reichman, P. N. Roy, S. Jang, and G. A. Voth, J. Chem. Phys. **113**, 919 (2000).
[25] E. Geva, Q. Shi, and G. A. Voth, J. Chem. Phys. **115**, 9209 (2001).
[26] N. Blinov and P. N. Roy, J. Chem. Phys. **115**, 7822 (2001).
[27] Q. Shi and E. Geva, J. Chem. Phys. **118**, 8173 (2003).
[28] Q. Shi and E. Geva, J. Chem. Phys. **119**, 9030 (2003).
[29] I. R. Craig and D. E. Manolopoulos, J. Chem. Phys. **121**, 3368 (2004).
[30] I. R. Craig and D. E. Manolopoulos, J. Chem. Phys. **122**, 084106 (2005).
[31] T. D. Hone and G. A. Voth, J. Chem. Phys. **121**, 6412 (2004).
[32] A. Nakayama and N. Makri, Proc. Natl. Acad. Sci. U.S.A. **102**, 4230 (2005).
[33] F. J. Webster, P. J. Rossky, and R. A. Friesner, Comput. Phys. Commun. **63**, 494 (1991).
[34] F. J. Webster, J. Schnitker, M. S. Friedrichs, R. A. Friesner, and P. J. Rossky, Phys. Rev. Lett. **66**, 3172 (1991).
[35] E. J. Heller, J. Chem. Phys. **65**, 1289 (1976).
[36] X. Sun, H. B. Wang, and W. H. Miller, J. Chem. Phys. **109**, 7064 (1998).
[37] X. Sun and W. H. Miller, J. Chem. Phys. **110**, 6635 (1999).
[38] H. B. Wang, M. Thoss, and W. H. Miller, J. Chem. Phys. **112**, 47 (2000).
[39] K. Thompson and N. Makri, J. Chem. Phys. **110**, 1343 (1999).
[40] N. Makri, J. Phys. Chem. A **108**, 806 (2004).
[41] J. A. Poulsen, G. Nyman, and P. J. Rossky, J. Chem. Phys. **119**, 12179 (2003).
[42] L. S. Schulman, *Techniques and Applications of Path Integration* (Wiley, New York, 1981).
[43] S. S. Zhang and E. Pollak, J. Chem. Phys. **119**, 11058 (2003).
[44] A. A. Golosov and D. R. Reichman, J. Chem. Phys. **114**, 1065 (2001).
[45] E. Rabani and D. R. Reichman, Phys. Rev. E **65**, 036111 (2002).
[46] D. R. Reichman and E. Rabani, Phys. Rev. Lett. **87**, 265702 (2001).
[47] E. Rabani and D. R. Reichman, J. Chem. Phys. **116**, 6271 (2002).
[48] D. R. Reichman and E. Rabani, J. Chem. Phys. **116**, 6279 (2002).
[49] E. Rabani and D. R. Reichman, Europhys. Lett. **60**, 656 (2002).
[50] E. Rabani, AIP Conf. Proc. **690**, 281 (2003).
[51] E. Rabani and D. R. Reichman, J. Chem. Phys. **120**, 1458 (2004).
[52] E. Rabani, K. Miyazaki, and D. R. Reichman, J. Chem. Phys. **122**, 034502 (2005).
[53] E. Rabani and D. R. Reichman, J. Phys. Chem. B **105**, 6550 (2001).
[54] G. D. Mahan, *Many-Particle Physics* (Plenum, New York, 2000).
[55] A. L. Fetter and J. D. Walecka, *Quantum Theory of Many Particle Systems* (McGraw-Hill, New York, 1971).
[56] J. W. Negele and H. Orland, *Quantum Many-Particle Systems* (Addison-Wesley, New York, 1992).
[57] T. Van Voorhis and D. R. Reichman, J. Chem. Phys. **120**, 579 (2004).
[58] T. Frabisch, M. Fuchs, W. W. Götze, and A. P. Singh, Phys. Rev. E **56**, 5659 (1997).
[59] S. H. Chong and F. Hirata, Phys. Rev. E **58**, 7296 (1998).
[60] U. Balucani and M. Zoppi, *Dynamics of the Liquid State* (Oxford, New York, 1994).
[61] J. P. Boon and S. Yip, *Molecular Hydrodynamics* (McGraw-Hill, New York, 1980).
[62] J. P. Hansen and I. R. McDonald, *Theory of Simple Liquids* (Academic, San Diego, 1986).
[63] J. E. Gubernatis, M. Jarrell, R. N. Silver, and D. S. Silvia, Phys. Rev. B **44**, 6011 (1991).
[64] C. E. Creffield, E. G. Klepfish, E. R. Pike, and S. Sarkar, Phys. Rev. Lett. **75**, 517 (1995).
[65] E. Gallicchio and B. J. Berne, J. Chem. Phys. **101**, 9909 (1994).
[66] E. Gallicchio and B. J. Berne, J. Chem. Phys. **105**, 7064 (1996).
[67] M. Boninsegni and D. M. Ceperley, J. Low Temp. Phys. **104**, 339 (1996).
[68] D. Kim, J. D. Doll, and D. L. Freeman, J. Chem. Phys. **108**, 3871 (1998).
[69] S. A. Egorov, E. Gallicchio, and B. J. Berne, J. Chem. Phys. **107**, 9312 (1997).
[70] E. Gallicchio, S. A. Egorov, and B. J. Berne, J. Chem. Phys. **109**, 7745 (1998).
[71] E. Rabani, G. Krilov, and B. J. Berne, J. Chem. Phys. **112**, 2605 (2000).
[72] E. Sim, G. Krilov, and B. J. Berne, J. Phys. Chem. A **105**, 2824 (2001).
[73] E. Rabani, D. R. Reichman, G. Krilov, and B. J. Berne, Proc. Natl. Acad. Sci. U.S.A. **99**, 1129 (2002).
[74] A. A. Golosov, D. R. Reichman, and E. Rabani, J. Chem. Phys. **118**, 457 (2003).
[75] D. Kim, J. D. Doll, and J. E. Gubernatis, J. Chem. Phys. **106**, 1641 (1997).
[76] D. M. Ceperley, Rev. Mod. Phys. **67**, 279 (1995).
[77] J. A. Poulsen, G. Nyman, and P. J. Rossky, J. Phys. Chem. B **108**, 19799 (2004).
[78] R. Zwanzig, *Lectures in Theoretical Physics* (Wiley, New York, 1961), Vol. III, p. 135.
[79] H. Mori, Prog. Theor. Phys. **33**, 423 (1965).
[80] H. Mori, Prog. Theor. Phys. **34**, 399 (1965).
[81] B. J. Berne and G. D. Harp, Adv. Chem. Phys. **17**, 63 (1970).
[82] R. Kubo, M. Toda, and N. Hashitsume, *Statistical Physics II*, Springer Series in Solid-State Sciences, 2nd ed. (Springer, Berlin, 1995).
[83] D. B. Woods, E. C. Svensson, and P. Martel, Can. J. Phys. **56**, 302 (1978).
[84] In the original derivation (Ref. 73) the self-diffusion constant is related to $D(\omega)/6$ since we work with the velocity vector, while here we work with one of its components.
[85] B. J. Berne, J. Stat. Phys. **43**, 911 (1986).
[86] B. J. Berne and D. Thirumalai, Annu. Rev. Phys. Chem. **37**, 401 (1986).
[87] *Maximum Entropy and Bayesian Methods*, edited by J. Skilling (Kluwer, Cambridge, England, 1989).
[88] C. L. Lawson and R. J. Hanson, *Solving Least Squares Problems* (Society for Industrial and Applied Mathematics, Philadelphia, 1995).
[89] S. Miura, S. Okazaki, and K. Kinugawa, J. Chem. Phys. **110**, 4523 (1999).
[90] J. A. Poulsen, G. Nyman, and P. J. Rossky, J. Phys. Chem. A **108**, 8743 (2004).
[91] E. L. Pollock and D. M. Ceperley, Phys. Rev. B **30**, 2555 (1984).
[92] R. A. Aziz, M. J. Slaman, A. Koide, A. R. Allnatt, and W. J. Meath, Mol. Phys. **77**, 321 (1992).
[93] N. Makri (unpublished).